Journal of Applied Polymer Science

# Phosphorous, nitrogen co-doped carbon from spent coffee grounds for fuel cell applications

**Sunil Kumar Ramasahayam, Saad Azam, Tito Viswanathan**
Department of Chemistry, University of Arkansas at Little Rock, 2801 S. University Ave, Little Rock, Arkansas 72204
Correspondence to: S. K. Ramasahayam (E-mail: sxramasahaya@ualr.edu) and T. Viswanathan (E-mail: txviswanatha@ualr.edu)

**ABSTRACT:** Spent coffee grounds, which represents the vast solid residual matter generated from consumed coffee beans, requires proper reutilization. This work represents the production of an alternate material from spent coffee grounds to replace expensive metal based catalysts currently used as electrodes in fuel cells. A novel microwave assisted technique which is easy, rapid, and economical is utilized for the synthesis of Phosphorous, Nitrogen co-doped carbon (PNDC) from spent coffee grounds and ammonium polyphosphate. SEM analysis revealed that PNDC is composed of distinct, spherical shaped particles. PNDC has a BET surface area of ~507 $m^2$ $g^{-1}$ and is predominantly mesoporous. XPS reveals that PNDC contains about 1.90% N and 3.02% P besides C and O. PNDC exhibits good $O_2$ reduction response in 0.1*M* KOH, which was found to be comparable to that of 20% Pt/C. © 2015 Wiley Periodicals, Inc. J. Appl. Polym. Sci. **2015**, *132*, 41948.

**KEYWORDS:** applications; batteries and fuel cells; electrochemistry; morphology; porous materials

Received 15 October 2014; accepted 2 January 2015
**DOI: 10.1002/app.41948**

## INTRODUCTION

Today, coffee is one of the most widely consumed beverages all over the world. According to the "International Coffee Organization," the production of coffee for the year 2008, accounted to about 680,000,000 tons.[1] Every year, the production continues to increase to keep pace with the growing consumer demands. Proportionately, spent coffee grounds (the solid residue left after treating coffee grounds with hot water) generation, tends to increase. Taking into consideration the enormous amounts of wastes generated from coffee making, a greater threshold exists to dispose them off efficiently. Spent coffee grounds are mainly being utilized for the production of biodiesel and fuel pellets.[2] They are also being used for making inexpensive and cheap adsorbents for the removal of dyes, lead ions etc. from waste waters.[3,4]

Different kinds of nitrogen precursors have been utilized to achieve nitrogen doping in carbon which include ethylenediamine,[5,6] diaminopropane,[7] cyanamide,[8] dicyandiamide,[9] ionic liquids,[5] etc. But, these sources of nitrogen are deemed toxic to humans. Therefore, a very high threshold exists to find an alternate inexpensive, green nitrogen precursor for the synthesis of nitrogen doped mesoporous carbon. Spent coffee grounds are an excellent green source of N. Coffee grounds contain about 2.56% N and 51.31% C with a C to N ratio of about 24 : 1.[10,11] Therefore, we decided to utilize spent coffee grounds as an inexpensive, green, abundant precursor for preparing Phosphorous, Nitrogen co-doped carbon (PNDC). Ammonium polyphosphate, which is a good microwave absorber was used as the dehydrating agent and also serves as a source for N (besides spent coffee grounds) and P dopants.

Heteroatom doped carbons find a wide array of applications including energy storage and conversion,[12–15] electrocatalysis,[16,17] sensors,[18–20] and electronics.[21–23] The current study is the use of novel heteroatom doped carbon produced from spent coffee grounds as fuel cell electrodes. Fuel cells are considered to be promising alternative energy sources because of their high efficiency, cleanliness, and flexibility for different applications.[24–29] The efficiency of a fuel cell strongly depends upon the oxygen reduction reaction (ORR) at the cathode.[30] Several catalysts are available for ORR at cathode. Pt and its alloys are considered as the best ORR catalysts known so far. However, the high cost and scarcity of Pt, solubility and agglomeration problems associated with Pt, render these fuel cells commercially unviable.[31–34]

Recently, hetero-atom doped carbons such as carbon spheres, ordered mesoporous graphitic arrays, carbon nanotubes, and

This article was published online on 23 January 2015. An error was subsequently identified. This notice is included in the online and print versions to indicate that both have been corrected 31 Jan 2015.

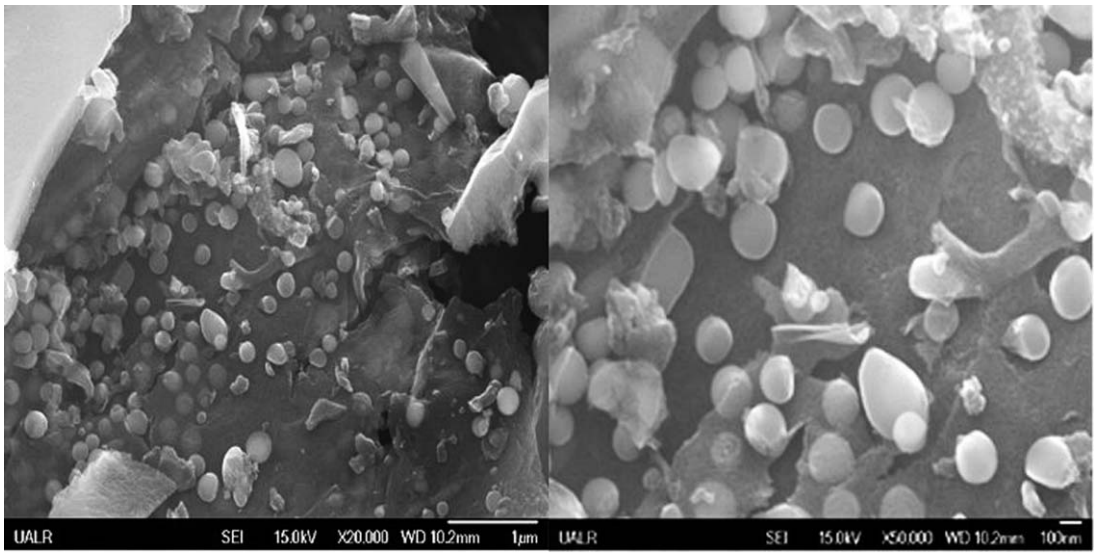


**Figure 1.** Scanning electron microscopic images of PNDC at (a) ×20,000 magnification and (b) ×50,000 magnification.

ordered mesoporous carbon[29,35–41] are gaining increasing attention as ORR catalysts. These carbon based catalysts are relatively inexpensive, environmentally friendly and exhibit superior electrochemical performance.[42–47] Among these carbon based catalysts, doped mesoporous carbon could be most suited for ORR applications in fuel cells owing to their uniform porous structure, large specific pore volume and a high specific surface area.[48,49]

Different techniques have been reported to be useful in the synthesis of doped carbon materials. Chemical vapor deposition,[50–52] arc discharge,[53] thermal annealing,[54,55] and plasma methods[16] etc. are some techniques, to name a few. But, these methods employ complicated procedures utilizing either toxic gases or expensive instruments, are low yielding and are expensive.[56–58] Therefore, an interesting challenge lies to find a facile method for the synthesis of doped carbon materials. Recently, microwave-assisted synthesis has been shown to be viable for the synthesis of carbon based materials because it is rapid, can attain high temperatures in a short time, does not require any inert or reducing gases during synthesis and is environmental friendly.[58–63] A detailed description of microwave radiation and the treatment process has been described elsewhere by one of our co-authors.[64–66]

In this article, the synthesis and characterization of PNDC from spent coffee grounds is reported. The synthesized PNDC exhibited characteristics conducive for good ORR performance in alkaline conditions. Besides these applications, PNDC from coffee grounds may also be useful for environmental remediation related applications like organic dye degradation and removal of pollutants like phosphorous, arsenic, etc. from polluted waters.

## EXPERIMENTAL

### Materials

Spent coffee grounds were obtained from a local coffee shop. Ammonium polyphosphate was obtained from JLS Chemicals, China. Twenty percent Pt/C was purchased from Clean Fuel Cell Energy, LLC. All the chemicals obtained were of analytical grade and were utilized without further purification.

### Synthesis of PNDC from Spent Coffee Grounds

A 1.0 g sample of dried and powdered spent coffee grounds were blended very well with 0.40 g of ammonium polyphosphate in a mortar and pestle. The mixture was subsequently exposed to microwave radiation in a boron nitride crucible with a similar cap in a muffle using a commercial table top microwave operating at 1.25 kW and 2.45 GHz for 30 min. The product was allowed to cool. The recovered product weighed $0.17 \pm 0.05$ g and was powdered using a mortar and pestle. The synthesized material was found to be conductive.

### Characterization of PNDC

Physical and chemical characteristics of the synthesized doped carbon materials were studied by different characterization techniques. Surface morphology was evaluated by JEOL 7000F Scanning Electron Microscopy. Thermo K-alpha X-ray Photoelectron

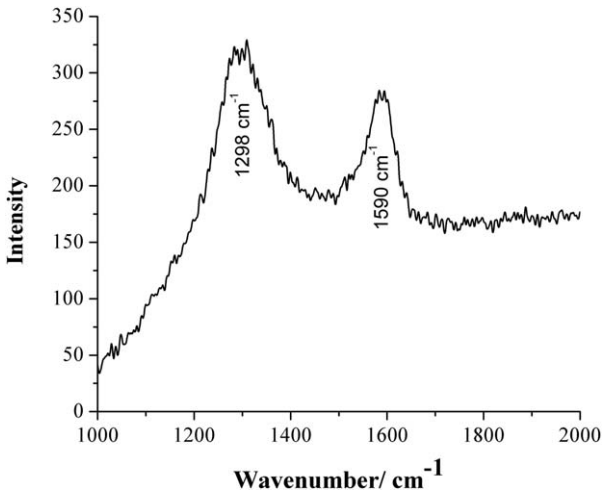


**Figure 2.** Raman spectrum of PNDC.

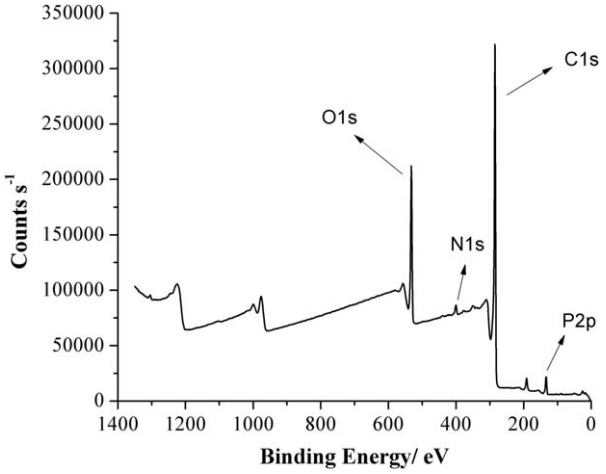


**Figure 3.** The survey spectrum of PNDC showing the presence of different elements.

Spectrometer (Source: Al K$\alpha$ radiation, 1486 eV, 12 kV, spot size: 200 $\mu$m, and carbon internal standard at 285.0 eV) was utilized to understand the nature and extent of doping in PNDC. Micromeritics Surface Area Analyzer ASAP-2020 was utilized to understand the surface area and pore characteristics of PNDC by nitrogen ($N_2$) sorption on powder samples at a bath temperature of 77.3 K. Horiba Jobin Yvon LabRam 800 equipped with 633 nm He-Ne laser was used to record Raman spectrum of PNDC.

**Table I.** Surface Elemental Composition of PNDC Determined Using XPS

| Carbon % (1s) | Oxygen % (O1s) | Nitrogen % (N1s) | Phosphorous % (P2p) |
|---|---|---|---|
| 78.90 | 16.00 | 1.90 | 3.02 |

### Electrochemical Methods

All cyclic voltammetric studies were performed using AFCBP1 bipotentiostat from Pine Instrument Company using a three electrode system at a scan rate of 100 mV $s^{-1}$. For rotating disk electrode (RDE) and rotating ring disk electrode (RRDE) studies performed at a scan rate of 20 mV $s^{-1}$ and 50 mV $s^{-1}$, respectively between a potential range of −800 and 200 mV, a MSRX electrode rotator from Pine Instrument Company was used in conjugation with the AFCBP1 bipotentiostat. All electrochemical studies were performed in a freshly prepared 0.1*M* KOH electrolytic solution using Hg/HgO as the reference electrode and Pt wire as the counter electrode. A glassy carbon electrode (5 mm diameter and 0.196 $cm^2$ geometric area) in polytetrafluoroethylene holder was chosen as the working

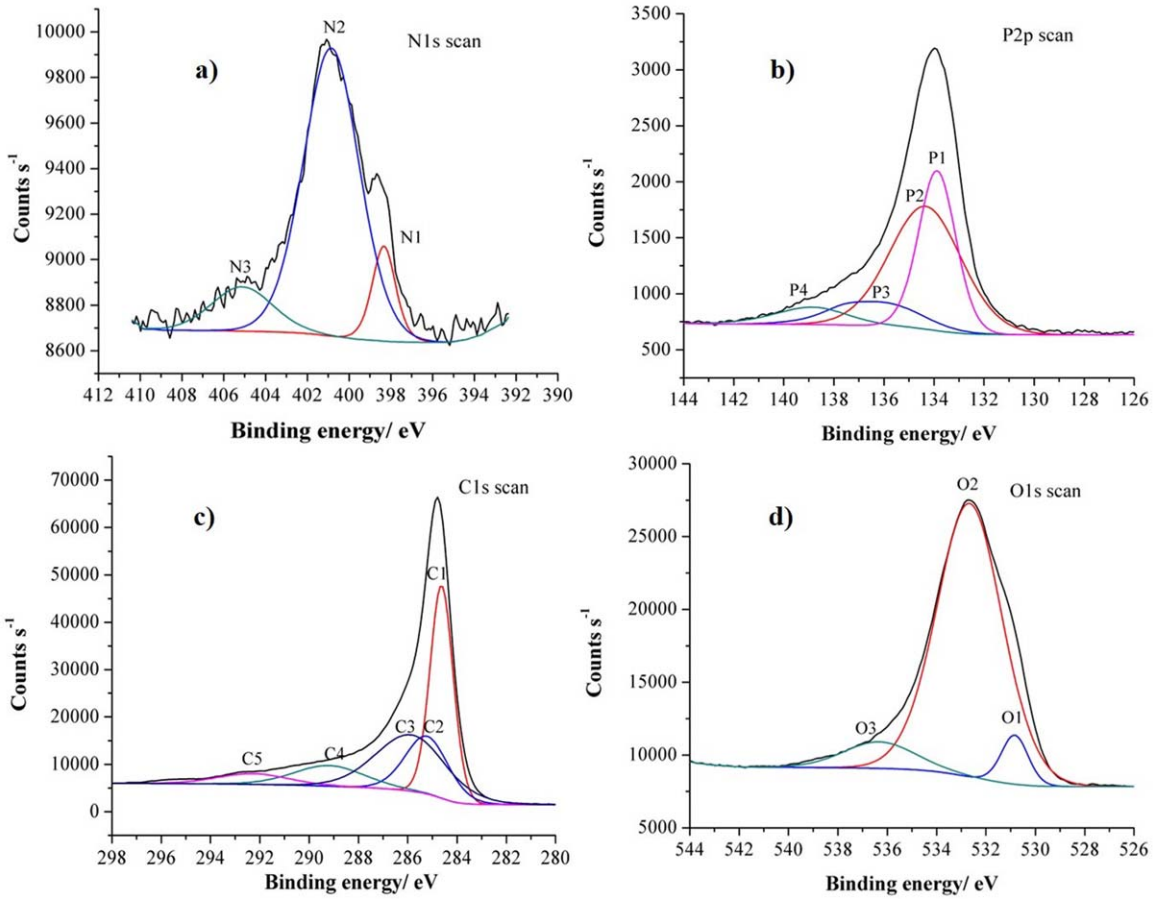


**Figure 4.** The fitted XPS peaks of PNDC. (a) The fitted peaks of N, (b) the fitted peaks of P, (c) the fitted peaks of C, and (d) the fitted peaks of O. [Color figure can be viewed in the online issue, which is available at wileyonlinelibrary.com.]

**Table II.** The Results from Peak Fitting Analysis of PNDC

| Peaks | Peak BE (eV) | Atomic (%) | Peaks | Peak BE (eV) | Atomic (%) | Peaks | Peak BE (eV) | Atomic (%) | Peaks | Peak BE (eV) | Atomic (%) |
|---|---|---|---|---|---|---|---|---|---|---|---|
| C1 | 284.7 | 35.7 | N1 | 398.3 | 10.7 | P1 | 133.9 | 32.5 | O1 | 530.83 | 6.2 |
| C2 | 285.3 | 18.2 | N2 | 400.9 | 76.4 | P2 | 134.3 | 49.8 | O2 | 532.67 | 84.9 |
| C3 | 286.0 | 29.0 | N3 | 404.8 | 12.8 | P3 | 137.0 | 11.2 | O3 | 536.29 | 8.9 |
| C4 | 289.3 | 10.6 | | | | P4 | 139.6 | 6.5 | | | |
| C5 | 292.4 | 5.6 | | | | | | | | | |

electrode. For ORR studies, the electrolyte was purged with $O_2$ for at least 30 min prior to the measurements and continuous $O_2$ flow above the electrolyte was maintained to create an $O_2$ blanket. The glassy carbon electrode was cleaned several times using distilled water followed by polishing the surface using 0.05 $\mu$m alumina. A 10 mL of 1 mg $mL^{-1}$ suspension of PNDC from spent coffee grounds was prepared by sonication for 60 min. To 0.5 mL of this dispersion, 20 $\mu$L of nafion was added and sonicated for 10 min. A 20 $\mu$L of the resulting dispersion was drop-casted onto glassy carbon electrode, air dried, and this PNDC modified glassy carbon electrode was utilized as working electrode for electrochemical studies. Similarly, for comparison, a 10 mL of 1 mg $mL^{-1}$ suspension of 20% Pt/C in ethanol was prepared by sonication for 1 h. To 0.5 mL of the prepared suspension, 20 $\mu$L Nafion was added and sonicated for 10 min. A 20 $\mu$L of prepared suspension was utilized to prepare Pt/C modified glassy carbon electrode in a similar manner reported earlier.

## RESULTS AND DISCUSSION

### Scanning Electron Microscopy

Scanning Electron Microscopic (SEM) images were recorded to understand the morphology (size and shape) of the material. SEM images at different magnifications can be seen in Figure 1. Clear spherical shaped particles are formed which are interspersed in the carbon matrix. Size of the particles ranges from 100 nm to a few hundred nanometers.

### Raman Spectroscopy

Figure 2 shows the Raman spectrum of PNDC from spent coffee grounds. The Raman spectrum shows two prominent peaks, one at 1298 $cm^{-1}$ and the other at 1590 $cm^{-1}$. The peak at 1298 $cm^{-1}$ represents the D band or the disordered band and the peak at 1590 $cm^{-1}$ represents the G band or the graphitic band. The D-band is indicative of the breathing mode of the $sp^2$ rings of the graphene layer that is related to a series of defects as a result of heteroatom doping, whereas the G-band is the result of the in-plane bond-stretching motion of pairs of $sp^2$ C-atoms.[67–69] The ratio of intensities of the D band and the G band is 1.16, which is indicative of the extent of disordered carbon in PNDC.

### X-ray Photoelectron Spectroscopy (XPS)

The survey spectrum of PNDC synthesized from spent coffee grounds is shown in Figure 3. The synthesized material is predominantly C and O with small amounts of N and P. The surface elemental composition is listed in Table I.

Figure 4 shows the fitted spectra of N, P, C, and O in PNDC. The fitted spectrum of N [Figure 4(a)] shows the presence of three different N bonding environments namely N1 (pyridinic; atomic % 10.73), N2 (pyrrolic/quarternary; atomic % 76.42), and N3 (pyridinic N-oxide; atomic % 12.84).[70–72] The deconvoluted spectrum of P [Figure 4(b)] shows four bonding environments namely P1, P2, P3, and P4. Only P1 and P2 are predominant, which are assigned to P—O (atomic % 32.52) and P—C (atomic % 49.81) bonding environments, respectively.[71,73,74] The fitted spectrum of C [Figure 4(c)] shows three main peaks C1, C2, and C3 conforming to graphitic/$sp^2$ C (atomic % 35.71), C—O/C=N (atomic % 18.20) and C=O (atomic % 29.03) bonding environments respectively.[56,57,72,73] O exists predominantly as O=C (atomic % 84.85) as seen in Figure 4(d).[16,70] The XPS analysis results are critical in understanding the characteristics of PNDC and correlating it to its performance. The results from the fitting of the peaks including peak binding energies, atomic % are summarized in Table II.

### Brunauer-Emmett-Teller (BET) Analysis

The surface area of PNDC synthesized from spent coffee grounds was determined to be 506.91 $m^2\ g^{-1}$ by BET method. On the basis of the BET results, PNDC can be classified as predominantly mesoporous, along with some micropores. BET analysis results are summarized in Table III.

The $N_2$ adsorption–desorption plot of PNDC can be seen in Figure 5. PNDC exhibits a Type IV isotherm according to IUPAC classification.[75] The material exhibits a characteristic monolayer-multilayer adsorption. The inflection point A, separates monolayer adsorption at lower relative pressures ($P/P_o$) from multilayer adsorption at higher relative pressures ($P/P_o$).

**Table III.** Summary of BET Analysis Results

| Sample | BET surface area ($m^2\ g^{-1}$) | Micropore volume ($cm^3\ g^{-1}$) | Mesopore volume ($cm^3\ g^{-1}$) | Total pore volume ($cm^3\ g^{-1}$) | Average pore width (Å) | Average pore diameter (Å) |
|---|---|---|---|---|---|---|
| PNDC | 506.9 | 0.06 | 0.26 | 0.32 | 25.3 | 35.4 |

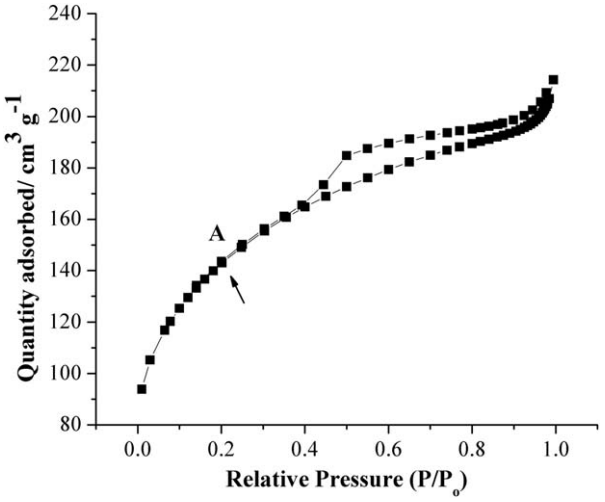


**Figure 5.** $N_2$ adsorption–desorption isotherm of PNDC.

The hysteresis loop observed can be described as a Type H4 according to IUPAC classification.[75,76] Type H4 loop is associated with narrow slit-like pores.

### Electrochemical Performance

The typical voltammograms displaying the $O_2$ reduction performance of PNDC in 0.1*M* KOH versus Hg/HgO reference electrode at a scan rate of 100 mV $s^{-1}$ can be seen in Figure 6. A clear sharp $O_2$ reduction peak can be seen at −0.379 V. The shape of the cyclic voltammogram appears to be perfectly rectangular exhibiting high current density. However, no such reduction peak could be observed in the absence of $O_2$ (the electrolyte being purged with $N_2$ to ensure the absence of $O_2$ in this case) as seen in Figure 6. This signifies the enormous potential of PNDC in reducing $O_2$. Also, the $O_2$ reduction performance of PNDC was compared to commercial 20% Pt/C, as seen in Figure 7. A 20% Pt/C exhibits an onset reduction potential of −0.09 V whereas PNDC exhibits an onset reduction potential of −0.17 V with current density close to that of 20% Pt/C. This signifies that PNDC synthesized from spent coffee grounds exhibits $O_2$ reduction performance comparable to commercial 20% Pt/C.

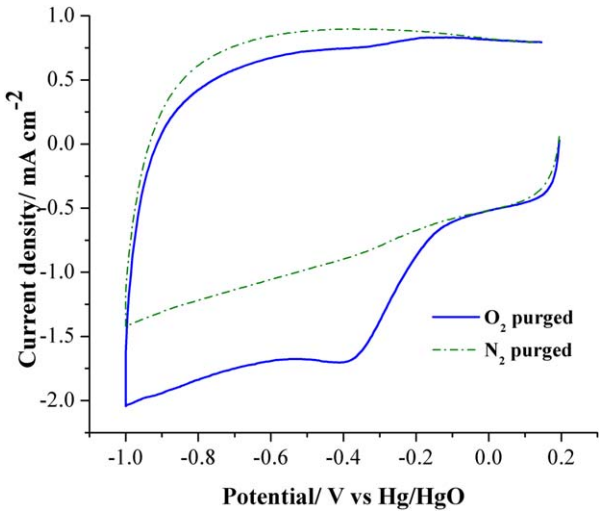


**Figure 6.** Cyclic voltammograms of PNDC in $O_2$ saturated and $N_2$ saturated 0.1*M* KOH at a scan rate of 100 mV $s^{-1}$. [Color figure can be viewed in the online issue, which is available at wileyonlinelibrary.com.]

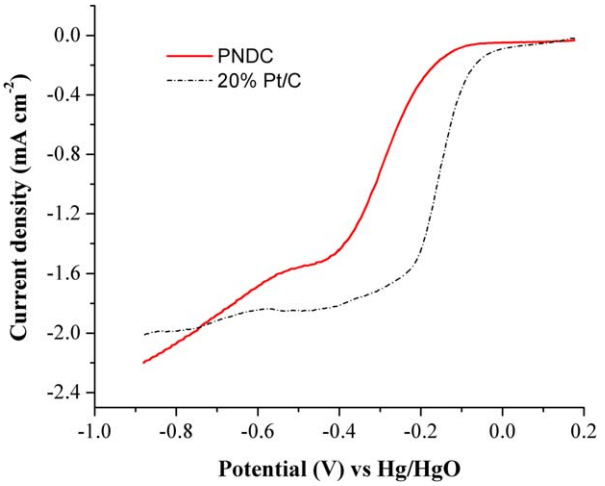


**Figure 7.** Linear sweep voltammograms of PNDC and 20% Pt/C in $O_2$ saturated 0.1*M* KOH at a rotation speed of 1600 rpm. [Color figure can be viewed in the online issue, which is available at wileyonlinelibrary.com.]

RDE studies were performed in $O_2$ saturated 0.1*M* KOH at a scan rate of 20 mV $s^{-1}$ to investigate the mechanism of $O_2$ reduction (a 4 $e^-$ or a 2 $e^-$ process) by PNDC. The RDE curves generated at different rotation speeds of 100, 400, 900, 1600, 2500 and 3600 rpm can be seen in Figure 8. Koutecky-Levich (K-L) equation[73,77,78] helps in calculating the number of electrons involved in the $O_2$ reduction process based on RDE curves. The K-L equation is as follows:

$$1/j_{lim} = 1/j_{ev} + 1/j_k$$

where $j_{lim}$, $j_{ev}$, and $j_k$ are the measured current density, Levich (or diffusion) current density and the kinetic current density,

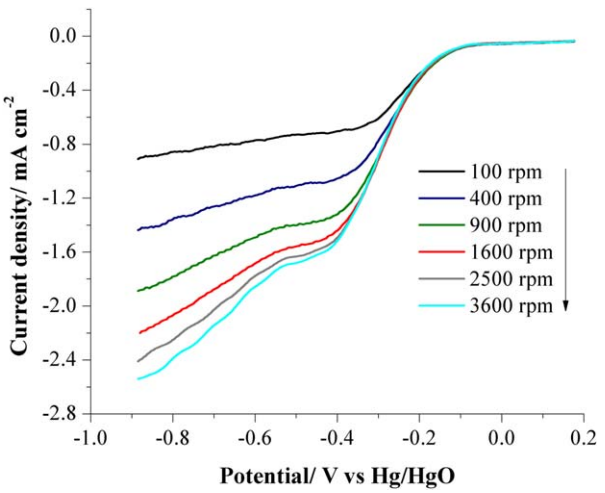


**Figure 8.** RDE studies of PNDC in $O_2$ saturated 0.1*M* KOH at different rotation speeds. [Color figure can be viewed in the online issue, which is available at wileyonlinelibrary.com.]

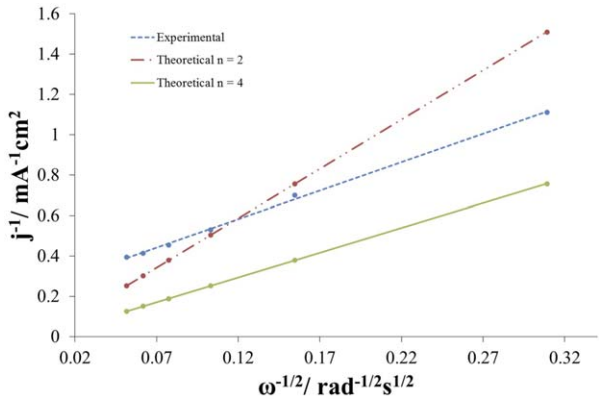


**Figure 9.** K–L plots of PNDC, theoretical 2 electron and 4 electron $O_2$ reduction processes. [Color figure can be viewed in the online issue, which is available at wileyonlinelibrary.com.]

respectively. $J_{lev}$ can be computed as 0.620 $nFCD^{2/3}\omega^{1/2}\upsilon^{-1/6}$ where, $n$ is the number of electrons involved in the process, $F$ is the Faraday constant ($F = 96485$ C $mol^{-1}$), C is the bulk concentration of $O_2$ ($C = 2.4 \times 10^{-4}$ M at 22°C), $D$ is the diffusion coefficient of $O_2$ in water at 22°C ($D = 1.7 \times 10^{-5}$ $cm^2$ $s^{-1}$), $\upsilon$ is the kinematic viscosity of the electrolyte at 22°C ($\upsilon = 0.01$ $cm^2$ $s^{-1}$), and $\omega$ is the angular velocity of the electrode ($\omega = 2\pi N$, where $N$ is the linear rotation speed).

A reciprocal of the square root of the angular rotation speed is plotted against the reciprocal of current density (calculated from the current generated at a particular point along each RDE curve) to yield a K-L plot for PNDC. Similar K-L plots were constructed for a theoretical 2 $e^-$ based $O_2$ reduction process and a 4 $e^-$ based $O_2$ reduction process for comparison. The resulting plots yielded straight lines with a slope [$1/(0.620\ nFCD^{2/3}\upsilon^{-1/6})$] and an intercept ($1/j_k$). The n value can be calculated from the slope of the straight line. All the K-L plots can be seen in Figure 9. The value of n for PNDC was determined to be 3.5, which is close to the theoretically proposed value of 4.

RRDE studies were performed in $O_2$ saturated 0.1$M$ KOH solution at a rotation speed of 2500 rpm, scan rate of 50 mV $s^{-1}$ and a voltage of 0.8 V. The RRDE voltammogram of PNDC can be seen in Figure 10. An almost zero ring current indicating no possible generation of $HO_2^-$ intermediate species[79,80] can be seen from Figure 10. Also, a very prominent disk current generation can be seen. This further confirms the mechanism of $O_2$ reduction by PNDC to be a 4 $e^-$ mediated process as indicated by the RDE results. The number of electrons involved in the ORR can also be computed from the RRDE studies based on the following equation:

$$n = 4I_D/(I_D + I_R/N)$$

where $n$ is the number of electrons involved in the reduction process, $I_D$ is the disk current, $I_R$ is the ring current, and $N$ is the collection efficiency of the electrode. On the basis of the results from RDE and RRDE studies, the overall mechanism of $O_2$ reduction by PNDC can be summarized as follows:

$$O_2 + 2\ H_2O + 4e^- \rightarrow 4OH^-$$

The high potential of PNDC synthesized from spent coffee grounds towards ORR can be attributed to the combined effect due to its high surface area, good porosity and appropriate amount of dopants. High surface area allows more of the reactive sites in PNDC to come in contact with the analyte moieties ($O_2$) and high porosity allows the analyte moieties to diffuse through the pores of the material and gain access to the reactive sites. The presence of N in PNDC renders adjacent C atoms electron deficient by virtue of its electronegativity and hence make adjacent C atoms as reactive sites towards ORR. Also, the dopant atoms like P being less electronegative than C, themselves act as harbor sites for $O_2$.[74,81–85]

To investigate the ability of PNDC to endure through long-term fuel cell applications, electrochemical stability studies were performed in $O_2$ saturated 0.1$M$ KOH at 100 mV $s^{-1}$. Figure 11 shows the cyclic voltammograms of PNDC before and after the generation of continuous 2000 cycles. The $O_2$ reduction

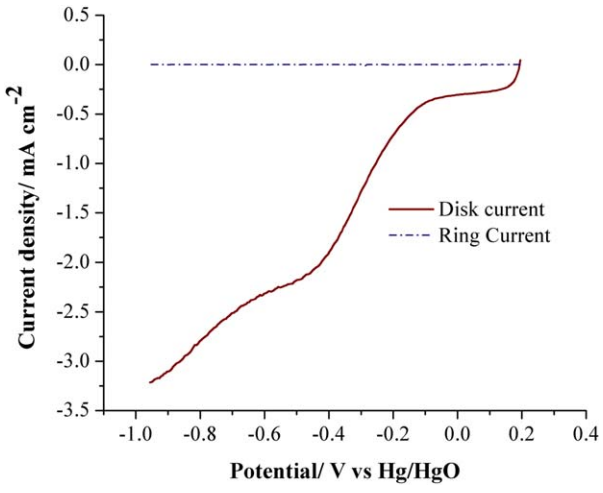


**Figure 10.** RRDE plot of PNDC in $O_2$ saturated 0.1$M$ KOH at rotation speed of 2500 rpm. [Color figure can be viewed in the online issue, which is available at wileyonlinelibrary.com.]

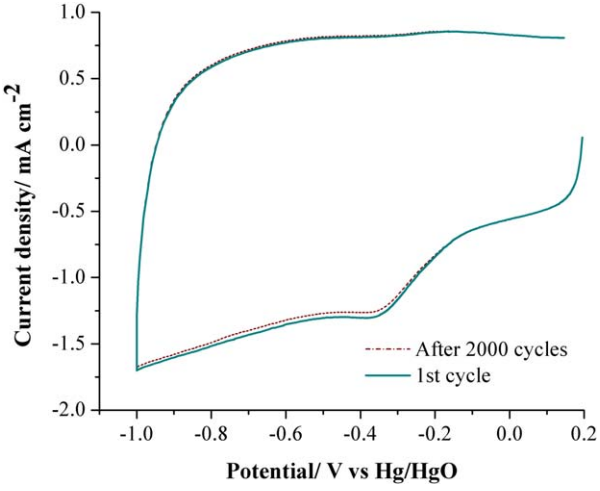


**Figure 11.** Cyclic voltammograms recorded before and after 2000 cycles to test the electrochemical stability of PNDC in $O_2$ saturated 0.1$M$ KOH at 100 mV $s^{-1}$. [Color figure can be viewed in the online issue, which is available at wileyonlinelibrary.com.]

performance of PNDC even after 2000 cycles is comparable to the performance during first cycle as only a very little loss in ORR activity could be observed over time.

## CONCLUSIONS

A novel renewable resource based material has been synthesized from spent coffee grounds. A robust microwave assisted method is made use of in the synthesis to yield a novel, economical, heteroatom-doped product (PNDC).

Some clear spherical shaped particles are formed from the carbon matrix ranging from 100 nm to a few hundred nanometers as evidenced by SEM. BET revealed the material to be highly porous with a surface area of 506.91 $m^2\ g^{-1}$. Raman spectroscopy indicates the presence of D-band and G-band respectively at 1298 and 1590 $cm^{-1}$ with $I_D/I_G$ ratio for PNDC greater than 1. XPS analysis reveals the presence of N, P, C, and O at 1.90%, 3.02%, 16.00%, and 78.90%, respectively.

PNDC exhibits an intense $O_2$ reduction peak in 0.1*M* KOH at −0.379 V and shows a high current density. The onset reduction potential and current density are comparable to commercial 20% Pt/C. The mechanism of $O_2$ reduction was found to be a 4 $e^-$ mediated process by RDE studies and no significant ring current was observed from RRDE studies in 0.1*M* KOH. The material was discovered to be highly stable for long-term practical fuel cell applications based on the electrochemical stability studies performed in 0.1*M* KOH. Thus, a potential means of successfully transforming an abundant daily waste (spent coffee grounds) to a commercially viable material (electrodes in fuel cells) has been demonstrated.

## ACKNOWLEDGMENTS

The authors would like to thank the Center for Integrative Nanotechnology Sciences at UALR for the equipment used in the characterization of the electrocatalyst. The authors would also like to acknowledge the partial financial support received through NASA Research Infrastructure Development grant.

## REFERENCES

1. Reffas, A.; Bernardet, V.; David, B.; Reinert, L.; Lehocine, M. B.; Dubois, M.; Batisse, N.; Duclaux, L. *J. Hazard. Mater.* **2010**, *175*, 779.
2. Kondamudi, N.; Mohapatra, S. K.; Misra, M. *J. Agric. Food Chem.* **2008**, *56*, 11757.
3. Franca, A. S.; Oliveira, L. S.; Ferreira, M. E. *Desalination* **2009**, *249*, 267.
4. Tokimoto, T.; Kawasaki, N.; Nakamura, T.; Akutagawa, J.; Tanada, S. *J. Colloid Interface Sci.* **2005**, *281*, 56.
5. Liu, R.; Wu, D.; Feng, X.; Muellen, K. *Angew. Chem.* **2010**, *49*, 2565, S2565/2561-S2565/2566.
6. Yang, S.; Feng, X.; Wang, X.; Muellen, K. *Angewandte Chem.* **2011**, *50*, 5339, S5339/5331-S5339/5339.
7. Higgins, D.; Chen, Z.; Chen, Z. *Electrochim. Acta* **2010**, *56*, 1570.
8. Kwon, K.; Sa, Y. J.; Cheon, J. Y.; Joo, S. H. *Langmuir* **2012**, *28*, 991.
9. Zhang, Y.; Fugane, K.; Mori, T.; Niu, L.; Ye, J. *J. Mater. Chem.* **2012**, *22*, 6575.
10. Cholakov, G.; Toteva, V.; Nikolov, R.; Uzunova, S.; Yanev, S. *J. Chem. Technol. Metall.* **2013**, *48*, 497.
11. Nídia, V. F. M. S.; Caetano, S.; Mata, T. M. *Chem. Eng. Trans.* **2012**, *26*.
12. Arranz-Andres, J.; Blau, W. J. *Carbon* **2008**, *46*, 2067.
13. Hino, T.; Ogawa, Y.; Kuramoto, N. *Fullerenes, Nanotubes, Carbon Nanostruct.* **2006**, *14*, 607.
14. Frackowiak, E.; Beguin, F. *Carbon* **2006**, *40*, 1775.
15. Fraysse, J.; Minett, A. I.; Jaschinski, O.; Duesberg, G. S.; Roth, S. *Carbon* **2002**, *40*, 1735.
16. Shao, Y.; Zhang, S.; Engelhard, M. H.; Li, G.; Shao, G.; Wang, Y.; Liu, J.; Aksay, I. A.; Lin, Y. *J. Mater. Chem.* **2010**, *20*, 7491.
17. Mo, Z.; Liao, S.; Zheng, Y.; Fu, Z. *Carbon* **2012**, *50*, 2620.
18. Chen, Y.-S.; Huang, J.-H.; Chuang, C.-C. *Carbon* **2009**, *47*, 3106.
19. Castro, M.; Lu, J.; Bruzaud, S.; Kumar, B.; Feller, J.-F. *Carbon* **2009**, *47*, 1930.
20. Hoa, N. D.; Van Quy, N.; Kim, D. *Sens. Actuators B* **2009**, *142*, 253.
21. Chen, F.; Xia, J.; Ferry, D. K.; Tao, N. *Nano Lett.* **2009**, *9*, 2571.
22. Wei, D.; Liu, Y.; Wang, Y.; Zhang, H.; Huang, L.; Yu, G. *Nano Lett.* **2009**, *9*, 1752.
23. Szafranek, B. N.; Fiori, G.; Schall, D.; Neumaier, D.; Kurz, H. *Nano Lett.* **2012**, *12*, 1324.
24. Zhang, L.; Zhang, J.; Wilkinson, D. P.; Wang, H. *J. Power Sources* **2006**, *156*, 171.
25. Bauen, A.; Hart, D. *J. Power Sources* **2000**, *86*, 482.
26. Luo, C.; Zuo, X.; Wang, L.; Wang, E.; Song, S.; Wang, J.; Wang, J.; Fan, C.; Cao, Y. *Nano Lett.* **2008**, *8*, 4454.
27. Arico, A. S.; Bruce, P.; Scrosati, B.; Tarascon, J.-M.; van Schalkwijk, W. *Nat. Mater.* **2005**, *4*, 366.
28. Wang, Y.; Chen, K. S.; Mishler, J.; Cho, S. C.; Adroher, X. C. *Appl. Energy* **2011**, *88*, 981.
29. Chen, Z.; Higgins, D.; Yu, A.; Zhang, L.; Zhang, J. *Energy Environ. Sci.* **2011**, *4*, 3167.
30. Bian, W.; Yang, Z.; Strasser, P.; Yang, R. *J. Power Sources* **2014**, *250*, 196.
31. Liu, Z.-W.; Peng, F.; Wang, H.-J.; Yu, H.; Zheng, W.-X.; Yang, J. *Angew. Chem.* **2011**, *50*, 3257, S3257/3251-S3257/3212.
32. Chen, W.; Chen, S. *Angew. Chem. Int. Ed.* **2009**, *48*, 4386.
33. Shao, Y.; Liu, J.; Wang, Y.; Lin, Y. *J. Mater. Chem.* **2009**, *19*, 46.
34. Liang, J.; Jiao, Y.; Jaroniec, M.; Qiao, S. Z. *Angew. Chem. Int. Ed.* **2012**, *51*, 11496.
35. Lyth, S. M.; Nabae, Y.; Moriya, S.; Kuroki, S.; Kakimoto, M.-A.; Ozaki, J.-I.; Miyata, S. *J. Phys. Chem. C* **2009**, *113*, 20148.
36. Biddinger, E. J.; Deak, D.; Ozkan, U. S. *Top. Catal.* **2009**, *52*, 1566.

37. Gong, K.; Du, F.; Xia, Z.; Durstock, M.; Dai, L. *Science* **2009**, *323*, 760.
38. Tang, Y.; Allen, B. L.; Kauffman, D. R.; Star, A. *J. Am. Chem. Soc.* **2009**, *131*, 13200.
39. Liu, G.; Li, X.; Ganesan, P.; Popov, B. N. *Appl. Catal. B* **2009**, *93*, 156.
40. Yu, D.; Zhang, Q.; Dai, L. *J. Am. Chem. Soc.* **2010**, *132*, 15127.
41. Sa, Y. J.; Park, C.; Jeong, H. Y.; Park, S.-H.; Lee, Z.; Kim, K. T.; Park, G.-G.; Joo, S. H. *Angew. Chem. Int. Ed.* **2014**, *53*, 4102.
42. Sidik, R. A.; Anderson, A. B.; Subramanian, N. P.; Kumaraguru, S. P.; Popov, B. N. *J. Phys. Chem. B* **2006**, *110*, 1787.
43. Gong, K.; Du, F.; Xia, Z.; Durstock, M.; Dai, L. *Science* **2009**, *323*, 760.
44. Pylypenko, S.; Mukherjee, S.; Olson, T. S.; Atanassov, P. *Electrochim. Acta* **2008**, *53*, 7875.
45. Matter, P. H.; Ozkan, U. S. *Catal. Lett.* **2006**, *109*, 115.
46. Choi, C. H.; Park, S. H.; Woo, S. I. *Green Chem.* **2011**, *13*, 406.
47. Jin, J.; Fu, X.; Liu, Q.; Liu, Y.; Wei, Z.; Niu, K.; Zhang, J. *ACS Nano* **2013**, *7*, 4764.
48. Zhou, M.; Shang, L.; Li, B.; Huang, L.; Dong, S. *Biosens. Bioelectron.* **2008**, *24*, 442.
49. Jun, S.; Joo, S. H.; Ryoo, R.; Kruk, M.; Jaroniec, M.; Liu, Z.; Ohsuna, T.; Terasaki, O. *J. Am. Chem. Soc.* **2000**, *122*, 10712.
50. Wei, G.; Wainright, J. S.; Savinell, R. F. *J. New Mater. Electrochem. Syst.* **2000**, *3*, 121.
51. Ledoux, M. J.; Vieira, R.; Pham-Huu, C.; Keller, N. *J. Catal.* **2003**, *216*, 333.
52. Matter, P. H.; Wang, E.; Arias, M.; Biddinger, E. J.; Ozkan, U. S. *J. Mol. Catal. A Chem.* **2007**, *264*, 73.
53. Panchakarla, L. S.; Govindaraj, A.; Rao, C. N. R. *Inorg. Chim. Acta* **2010**, *363*, 4163.
54. Schniepp, H. C.; Li, J.-L.; McAllister, M. J.; Sai, H.; Herrera-Alonso, M.; Adamson, D. H.; Prud'homme, R. K.; Car, R.; Saville, D. A.; Aksay, I. A. *J. Phys. Chem. B* **2006**, *110*, 8535.
55. Wang, X.; Li, X.; Zhang, L.; Yoon, Y.; Weber, P. K.; Wang, H.; Guo, J.; Dai, H. *Science* **2009**, *324*, 768.
56. Lin, Z.; Song, M.-K.; Ding, Y.; Liu, Y.; Liu, M.; Wong, C.-P. *Phys. Chem. Chem. Phys.* **2012**, *14*, 3381.
57. Lin, Z.; Waller, G.; Liu, Y.; Liu, M.; Wong, C.-P. *Adv. Energy Mater.* **2012**, *2*, 884.
58. Prasad, K. S.; Pallela, R.; Kim, D.-M.; Shim, Y.-B. *Part. Part. Syst. Charact.* **2013**, *30*, 557.
59. Das, S.; Mukhopadhyay, A. K.; Datta, S.; Basu, D. *Bull. Mater. Sci.* **2009**, *32*, 1.
60. Sathish-Kumar, K.; Vazquez-Huerta, G.; Rodriguez-Castellanos, A.; Poggi-Varaldo, H. M.; Solorza-Feria, O. *Int. J. Electrochem. Sci.* **2012**, *7*, 5484.
61. He, X.; Li, R.; Qiu, J.; Xie, K.; Ling, P.; Yu, M.; Zhang, X.; Zheng, M. *Carbon* **2012**, *50*, 4911.
62. Wang, C.; Wang, Y.; Zhan, L.; He, X.; Yang, J.; Qiao, W.; Ling, L. *Wuji Cailiao Xuebao* **2012**, *27*, 146.
63. Zheng, J.; Liu, H.-T.; Wu, B.; Di, C.-A.; Guo, Y.-L.; Wu, T.; Yu, G.; Liu, Y.-Q.; Zhu, D.-B. *Sci. Rep.* **2012**, *2*, 662/661.
64. Viswanathan, T. US Pat. 2013/0157838 A1 (**2011**).
65. Viswanathan, T.; Gunawan, G.; Bourdo, S.; Saini, V.; Moran, J.; Pack, L.; Owen, S. *J. Macromol. Sci. Part A: Pure Appl. Chem.* **2011**, *48*, 348.
66. Ramasahayam, S. K.; Gunawan, G.; Finlay, C.; Viswanathan, T. *Water Air Soil Pollut.* **2012**, *223*, 4853.
67. Ma, Y. W.; Zhang, L. R.; Li, J. J.; Ni, H. T.; Li, M.; Zhang, J. L.; Feng, X. M.; Fan, Q. L.; Hu, Z.; Huang, W. *Chin. Sci. Bull.* **2011**, *56*, 3583.
68. Paulus, U. A.; Wokaun, A.; Scherer, G. G.; Schmidt, T. J.; Stamenkovic, V.; Radmilovic, V.; Markovic, N. M.; Ross, P. N. *J. Phys. Chem. B* **2002**, *106*, 4181.
69. Rao, C. V.; Cabrera, C. R.; Ishikawa, Y. *J. Phys. Chem. Lett.* **2010**, *1*, 2622.
70. Bairi, V. G.; Bourdo, S. E.; Nasini, U. B.; Ramasahayam, S. K.; Watanabe, F.; Berry, B. C.; Viswanathan, T. *Sci. Adv. Mater.* **2013**, *5*, 1275.
71. Nasini, U. B.; Gopal Bairi, V.; Kumar Ramasahayam, S.; Bourdo, S. E.; Viswanathan, T.; Shaikh, A. U. *ChemElectroChem* **2014**, *1*, 573.
72. Chen, Z.; Higgins, D.; Chen, Z. *Carbon* **2010**, *48*, 3057.
73. Ramasahayam, S. K.; Nasini, U. B.; Bairi, V.; Shaikh, A. U.; Viswanathan, T. *RSC Adv.* **2014**, *4*, 6306.
74. Choi, C. H.; Park, S. H.; Woo, S. I. *ACS Nano* **2012**, *6*, 7084.
75. Kaneko, K. *J. Membr. Sci.* **1994**, *96*, 59.
76. Sing, K. S. W.; Everett, D. H.; Haul, R. A. W.; Moscou, L.; Pierotti, R. A.; Rouquerol, J.; Siemieniewska, T. *Pure Appl. Chem.* **1985**, *57*, 603.
77. Matter, P. H.; Zhang, L.; Ozkan, U. S. *J. Catal.* **2006**, *239*, 83.
78. Sun, Y.; Li, C.; Shi, G. *J. Mater. Chem.* **2012**, *22*, 12810.
79. Zheng, Y.; Jiao, Y.; Jaroniec, M.; Jin, Y.; Qiao, S. Z. *Small* **2012**, *8*, 3550.
80. Yu, D.; Nagelli, E.; Du, F.; Dai, L. *J. Phys. Chem. Lett.* **2010**, *1*, 2165.
81. Yu, D.; Xue, Y.; Dai, L. *J. Phys. Chem. Lett.* **2012**, *3*, 2863.
82. Zhang, M.; Dai, L. *Nano Energy* **2012**, *1*, 514.
83. Li, Y.; Huang, Z.; Huang, K.; Carnahan, D.; Xing, Y. *Energy Environ. Sci.* **2013**, *6*, 3339.
84. Maldonado, S.; Stevenson, K. J. *J. Phys. Chem. B* **2005**, *109*, 4707.
85. Wiggins-Camacho, J. D.; Stevenson, K. J. J. *Phys. Chem. C* **2011**, *115*, 20002.